



## Volumetric Ultrasound Imaging with Row-Column Addressed 2-D Arrays Using Spatial Matched Filter Beamforming

**Bouzari, Hamed; Engholm, Mathias; Christiansen, Thomas Lehrmann; Stuart, Matthias Bo; Nikolov, Svetoslav Ivanov; Thomsen, Erik Vilain; Thomsen, Erik Vilain; Jensen, Jørgen Arendt**

*Published in:*  
Proceedings of 2015 IEEE International Ultrasonics Symposium

*Link to article, DOI:*  
[10.1109/ULTSYM.2015.0497](https://doi.org/10.1109/ULTSYM.2015.0497)

*Publication date:*  
2015

*Document Version*  
Peer reviewed version

[Link back to DTU Orbit](#)

*Citation (APA):*  
Bouzari, H., Engholm, M., Christiansen, T. L., Stuart, M. B., Nikolov, S. I., Thomsen, E. V., Thomsen, E. V., & Jensen, J. A. (2015). Volumetric Ultrasound Imaging with Row-Column Addressed 2-D Arrays Using Spatial Matched Filter Beamforming. In *Proceedings of 2015 IEEE International Ultrasonics Symposium* IEEE. <https://doi.org/10.1109/ULTSYM.2015.0497>

---

### General rights

Copyright and moral rights for the publications made accessible in the public portal are retained by the authors and/or other copyright owners and it is a condition of accessing publications that users recognise and abide by the legal requirements associated with these rights.

- Users may download and print one copy of any publication from the public portal for the purpose of private study or research.
- You may not further distribute the material or use it for any profit-making activity or commercial gain
- You may freely distribute the URL identifying the publication in the public portal

If you believe that this document breaches copyright please contact us providing details, and we will remove access to the work immediately and investigate your claim.

# Volumetric Ultrasound Imaging with Row-Column Addressed 2-D Arrays Using Spatial Matched Filter Beamforming

Hamed Bouzari\*, Mathias Engholm<sup>†</sup>, Thomas Lehrmann Christiansen<sup>†</sup>, Matthias Bo Stuart\*, Svetoslav Ivanov Nikolov<sup>‡</sup>, Erik Vilain Thomsen<sup>†</sup> and Jørgen Arendt Jensen\*

\* Center for Fast Ultrasound Imaging, Dept. of Elec. Eng., Bldg. 349, Technical University of Denmark, 2800 Kgs. Lyngby, Denmark

<sup>†</sup> Dept. of Micro- and Nanotechnology, Technical University of Denmark, 2800 Kgs. Lyngby, Denmark

<sup>‡</sup> BK Ultrasound ApS, Herlev, Denmark

**Abstract**—For 3-D ultrasound imaging with row-column addressed 2-D arrays, the two orthogonal 1-D transmit and receive arrays are both used for one-way focusing in the lateral and elevation directions separately and since they are not in the same plane, the two-way focusing is the same as one-way focusing. However, the achievable spatial resolution and contrast of the B-mode images in Delay and Sum (DAS) beamforming are limited by the aperture size and by the operating frequency. This paper, investigates Spatial Matched Filter (SMF) beamforming on row-column addressed 2-D arrays to increase spatial resolution. The performance is investigated on both simulated and experimentally collected 3-D data by comparing the Point Spread Functions (PSFs) and the phantom images obtained with standard DAS and with SMF. Results show that the SMF beamformer outperforms DAS in both simulated and experimental trials and that a higher contrast resolution can be achieved by SMF beamforming (i.e., narrower main lobe and lower side lobes). The 6dB, 20dB and 40dB cystic resolution for a DAS simulated PSF at (0,0,30)mm are 1.22mm, 3.54mm and 7.46mm, for SMF beamforming they are 1.11mm, 2.33mm and 5.42mm accordingly. For measured RF-data of an iron needle facing toward the transducer positioned at (0,0,32.5)mm along the central axis, the 6dB, 20dB and 40dB cystic resolution for DAS beamforming are 1.99mm, 2.19mm and 4.26mm, and they are 0.8mm, 2.06mm and 4.18mm for SMF beamforming accordingly. SMF beamforming increases the contrast resolution which turns into a better quality of the B-mode images.

## I. INTRODUCTION

Real-time 3-D ultrasonic imaging requires, 2-D array transducers [1]. The number of elements in a fully addressed  $N \times N$  2-D array scales with  $N^2$ . A 1-D array with a penetration depth of around 300 - 400  $\lambda$  will for an  $f_{\#} = 2$  at a depth of 200  $\lambda$  require an aperture size of 64 - 100  $\lambda$ . This translates to 64 - 100 elements for a  $\lambda$ -pitch array, and 128 - 200 elements for a  $\frac{\lambda}{2}$ -pitch array. Using a fully addressed 2-D array, this would ideally correspond to an array with more than  $256^2$  elements. Moreover to control the individual elements in the array, a connection has to be made to each element. However, addressing each element individually results in a vast amount of interconnections and offers a great challenge in acquiring and processing the large amount of data. Reducing the number of transducer elements by using sparse arrays has therefore

attracted a great amount of interest in the last couple of decades. One of the drawbacks of sparse arrays, however, is the lower emitted energy from the reduced number of elements leading to a lower signal to noise ratio (SNR) in the recorded ultrasound image. The sparse arrays also have higher side-lobes and can introduce grating lobes in the field [2].

2-D row-column addressed arrays have recently received some attention [3]–[5]. In a row-column addressed array, the elements are accessed by their row or column index. Each row and column in the array thereby acts as one large element. This effectively transforms the dense 2-D array into two orthogonal 1-D arrays. This reduces the number of elements in an  $N \times N$  2-D array from  $N^2$  to  $2N$ . Since fewer interconnections are needed, the cost of the system design is reduced.

By row-column addressing the elements on a 2-D matrix array, each row or column is acoustically equivalent to a line-element. The long length of the line-elements results in prominent edge effects, which are due to the limited size of the aperture. It was shown that using hardware apodization along each row and column element, reduced those edge effects [6], [7]. In 3-D ultrasound imaging with row-column addressed 2-D arrays, the two orthogonal 1-D transmit and receive arrays are both used for focusing in the lateral and elevation directions separately. Even though it enables focusing in a 3-D volume, the spatial resolution of the two-way or transmit-receive focusing is equal to the one-way focusing in transmit or receive.

Spatial matched filter (SMF) beamforming is an algorithm, in which the impulse responses in transmission and in reception are considered for every point, unlike the DAS which assumes the impulse responses to be like delta functions [4], [8], [9]. Due to acoustically equivalent line-elements via row-column addressing the 2-D matrix array, SMF has the potential to improve the spatial resolution and the SNR. In [4], based on simulations, it was shown that SMF beamforming provides comparable results like synthetic aperture imaging with DAS beamforming. However this paper investigates SMF beamforming using synthetic aperture imaging.

In this study, Field II [10], [11] simulations are used to calculate the matched filter coefficients at all imaging points

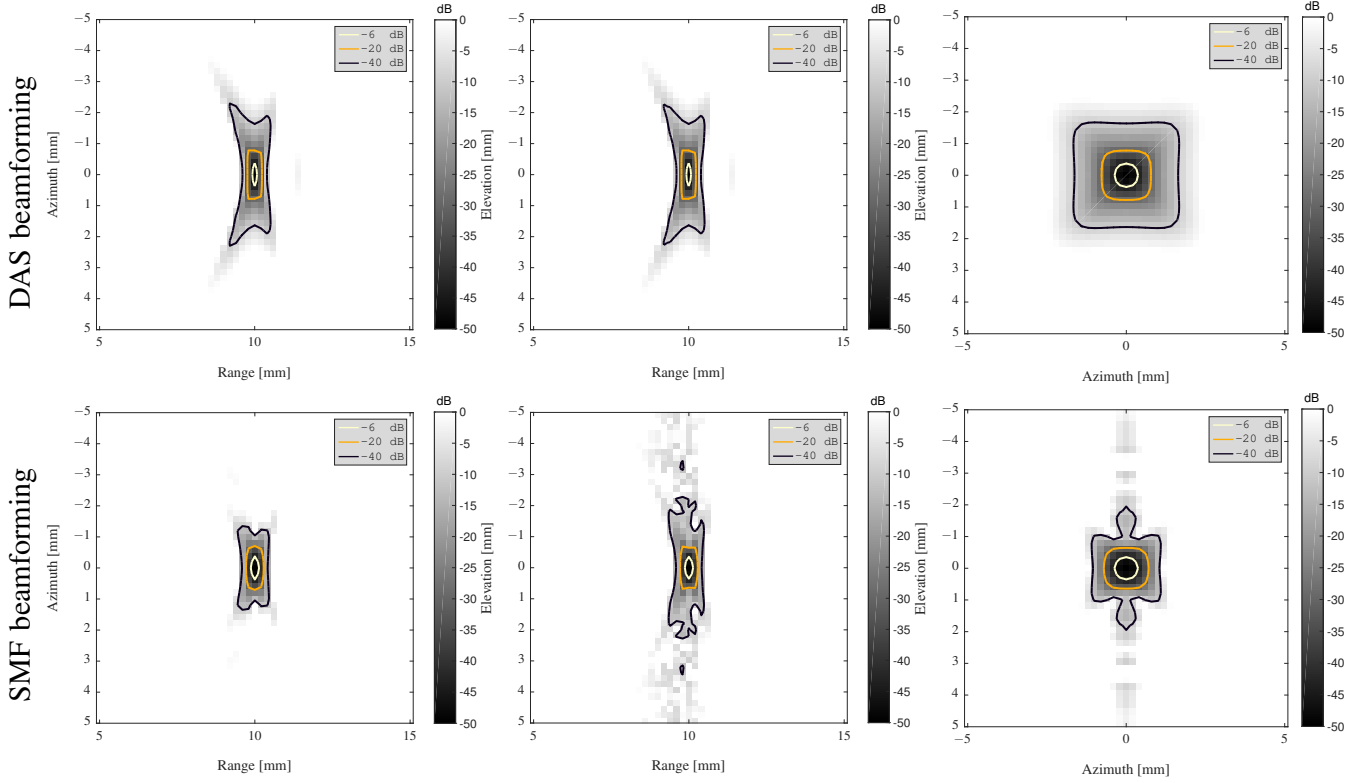


Fig. 1. Beamformed simulated PSFs of a scatterer positioned at (0,0,10) mm, using both SMF and DAS techniques. Roll-off apodization is applied along rows and columns. (single cycle excitation, synthetic aperture imaging over elevation direction, i.e. transmit direction. (Note that SMF is applied in lateral direction, i.e. receive direction))

instead of the analytical solution. This work also involves measurement of the impulse response of a prototype row-column array. Implementation of the SMF method is highly dependent on accurate measurements of the overall system impulse response to provide appropriate spatial filters.

This paper is organized as follows: First an introduction to the spatial matched filter beamforming is given. Afterwards, the measurement and simulation setups are explained. Finally, the B-mode images with both SMF and DAS algorithms are shown for the simulated and measured data. The last section concludes the paper.

## II. SPATIAL MATCHED FILTER BEAMFORMING

The signal from each channel of an array should be spatially matched filtered to align its output with that from the other channels so to add them constructively in phase. The received element signals are dependent on the element location and the scatterer's position, and a new matched filter must be used depending on the element and on the scatterer's position. The spatial matched filter  $m_p(\vec{r}_{trn}, \vec{r}_{rcv}, t)$  is then given by [12]:

$$\begin{aligned} m_p(\vec{r}_{trn}, \vec{r}_{rcv}, t) &= p_r(\vec{r}_{trn}, \vec{r}_{rcv}, -t) \\ p_r(\vec{r}_{trn}, \vec{r}_{rcv}, t) &= v_{pe}(t) *_{\vec{t}} h_t(\vec{r}_{trn}, \vec{r}_{rcv}, t) *_{\vec{t}} h_r(\vec{r}_{rcv}, \vec{r}_{trn}, t), \end{aligned} \quad (1)$$

which is dependent on the transmitter location  $\vec{r}_{trn}$ , the receiver element at  $\vec{r}_{rcv}$ , and the electro-mechanical impulse response of the transducer  $v_{pe}(t)$ . The impulse responses during transmission and reception are  $h_t(\vec{r}_{trn}, \vec{r}_{rcv}, t)$  and  $h_r(\vec{r}_{rcv}, \vec{r}_{trn}, t)$  for

the combined response for all of the array elements including their focusing and apodization. The focusing is then performed by adding the matched filtered signals from all the elements for the different locations

$$r_s(\vec{r}_i) = \sum_{j=1}^M \int_{t_{ij}}^{t_{ij} + \Delta T_{ij}} v_r(\vec{r}_j, t) p_r(\vec{r}_i, \vec{r}_j, t) dt, \quad (2)$$

where  $i$  designates the point in the image,  $j$  is the element number of the transducer,  $t_{ij}$  is the start of the response, and  $\Delta T_{ij}$  is the duration of the matched filter. The convolution integral in the equation is replaced by a correlation, since the time reversal of the response is replaced by the time reversal in the convolution.

It should be noticed that (2) can be used for any image point, and that it is only necessary to process the point in the image that must be displayed on the screen. The approach does not put any restrictions on the transducer geometry, excitation, focusing, apodization or impulse response. The approach can both be used for multi-element arrays and single element transducers, as long as the single element is moved compared to the scattering points during the imaging process in *e.g.* a polar scan. The approach improves on the focusing, if the pulse-echo spatial impulse responses are significantly different from a delta function. Normal delay focusing assumes that the geometric impulse response of the transducer is a delta function, and that the alignment can be done by merely delaying the responses. This is appropriate in the far-field for small element arrays and

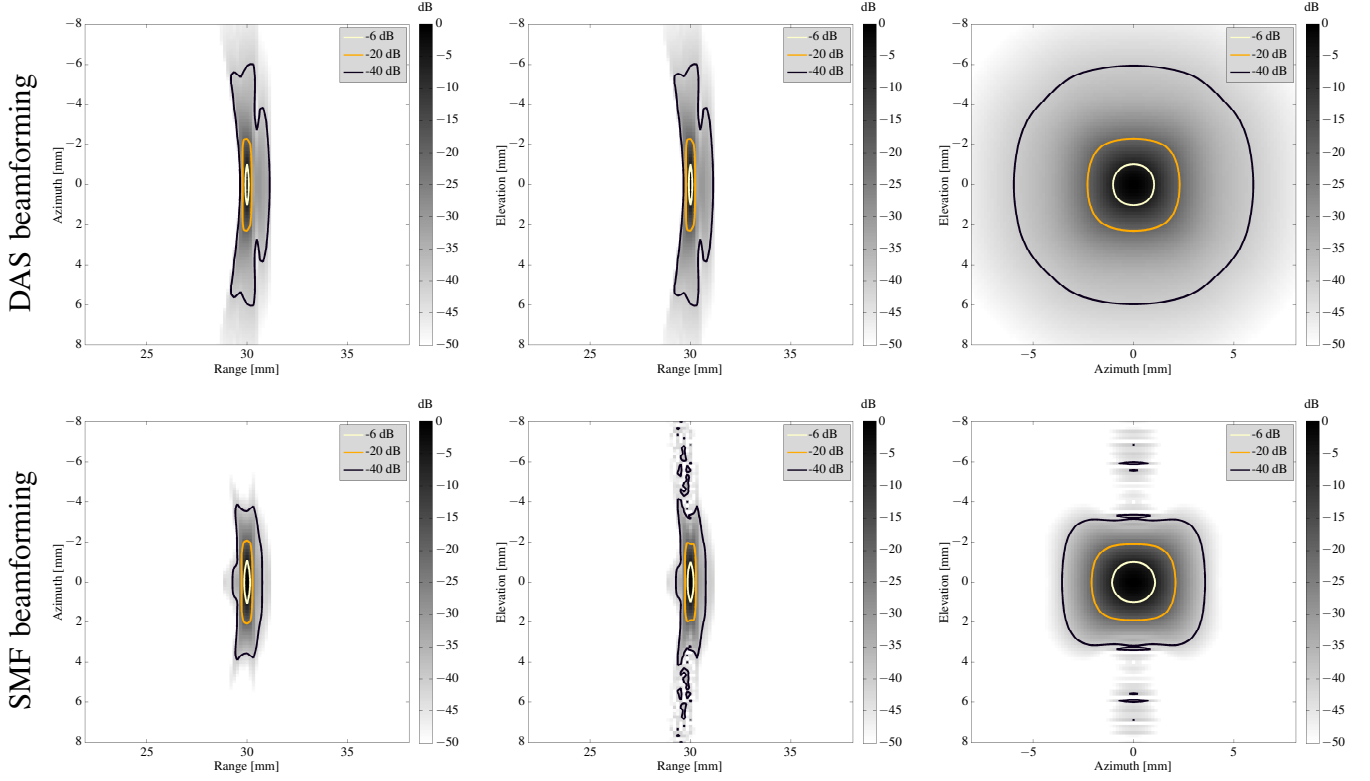


Fig. 2. Beamformed simulated PSFs of a scatterer positioned at (0,0,30) mm, using both SMF and DAS techniques. Roll-off apodization is applied along rows and columns. (single cycle excitation, synthetic aperture imaging over elevation direction, i.e. transmit direction. (Note that SMF is applied in lateral direction, i.e. receive direction))

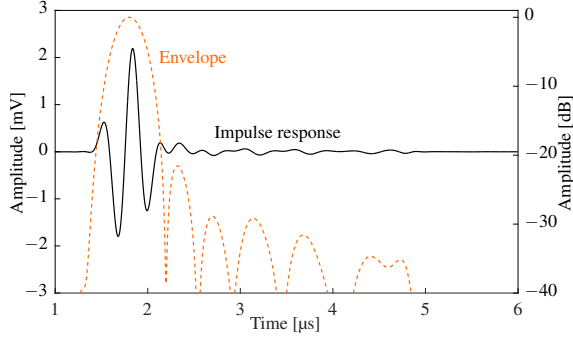


Fig. 3. Measured pulse-echo impulse response of the center column element, emitting with center row element. Note the two lobes after the main lobe which are due to the reflections from the shielding foil over the array.

at the focus for single element transducers. The approach will, thus, work best in the near field, where long spatial impulse responses are found. Specifically in row-column addressed 2-D arrays, where due to rather large elements the assumption of point sources for beamforming is inappropriate.

### III. SIMULATION AND MEASUREMENT SETUP

In this work, Field II is used for all simulations and also calculations of the spatial matched filters. The simulated receive signals are beamformed using two MATLAB (MathWorks Inc., Massachusetts, USA) specifically implemented DAS [7] and SMF beamformers for row-column addressed arrays. The

transducer arrays used in the simulations are row-column addressed 62+62 element 2-D arrays using the parameters shown in Table I. The receive array is rotated 90° with respect to the transmit array. Field II is set up to use lines to describe the apertures and each line-element is divided into square mathematical sub-elements with a side length of  $\lambda/4$ . Measurements are made with an in-house produced 62+62 element row-column addressed piezo array. An iron needle with a diameter of 300  $\mu\text{m}$  facing towards the transducer and along its center line, was used as a point target in a water bath.

Table I  
TRANSDUCER AND SIMULATION PARAMETERS.

Parameter name	Notation	Value	Unit
Number of elements	—	62+62	—
Center frequency	$f_0$	3.0	MHz
Speed of sound	$c$	1480	m/s
Wave length	$\lambda$	493.3	$\mu\text{m}$
Array pitch -x	$d_x$	$\lambda/2 = 246.6$	$\mu\text{m}$
Array pitch -y	$d_y$	$\lambda/2 = 246.6$	$\mu\text{m}$
Sampling frequency	$f_s$	120	MHz
Emission pulse	—	2-cycles, Hann-weighted	—

### IV. RESULTS

In Fig. 1, the simulated beamformed PSFs are shown for both SMF and DAS beamforming algorithms for a single cycle excitation with a roll-off apodization applied along each

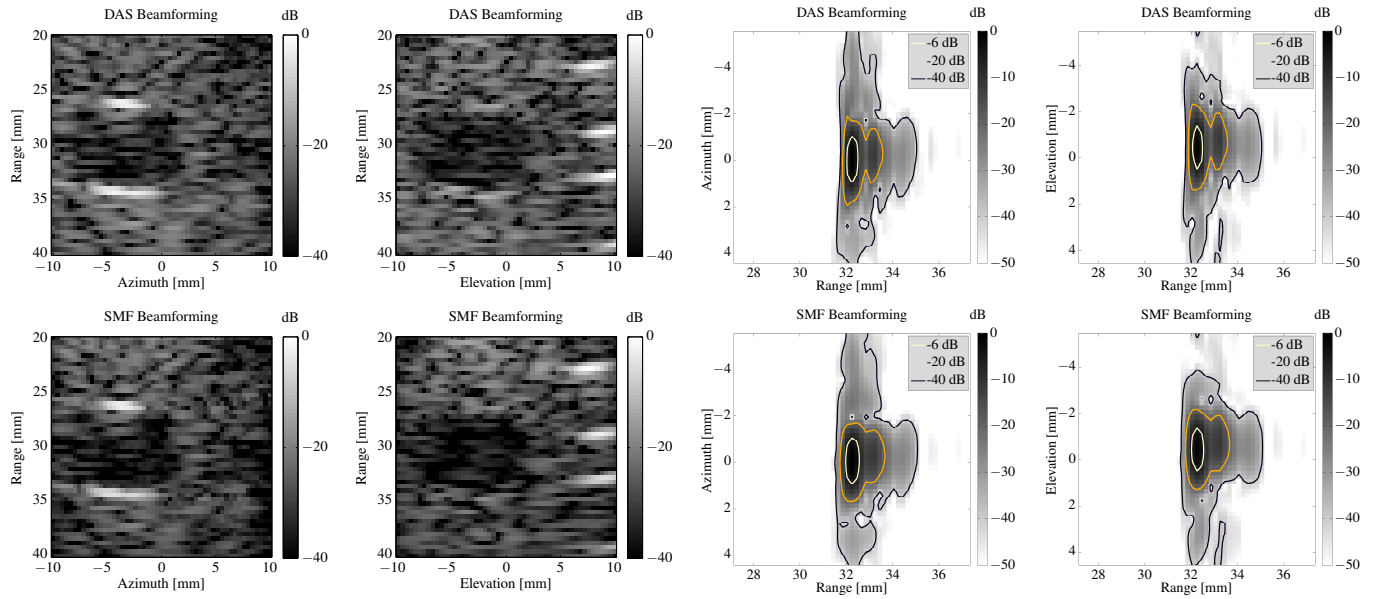


Fig. 4. Left two columns: Beamformed measured cyst phantom data using both SMF and DAS techniques. Right two columns: Beamformed measured PSFs of an iron needle facing toward the transducer positioned at the depth of 32.5mm along the central axis, using both SMF and DAS techniques.

row and column (scatterer positioned at (0,0,10) mm). The secondary echoes are suppressed more efficiently with SMF comparing to DAS beamforming. Although the contrast has clearly improved, the spatial resolution still stays the same as DAS. In Fig. 2, the simulated beamformed PSFs are shown for a scatterer positioned at (0,0,30) mm. Fig. 4 illustrates the beamformed PSF images of measured RF-data of an iron needle positioned at (0,0,32.5)mm in front of the transducer. The probe had roll-off hardware apodization turned on, therefore the edge echoes are not visible on the final beamformed images. However, those secondary echoes are due to the reflection of shielding foil, which was covered the array. The measured pulse-echo impulse response of the row-column probe, which is shown in Fig. 3, has been used for the SMF beamforming. Fig. 4 also illustrates the performance of DAS and SMF beamforming on a cyst phantom measured data.

## V. CONCLUSION

In this paper we demonstrate that the SMF beamforming algorithm is successfully employed for ultrasound B-mode image formation. Results of both simulated and experimental B-mode scans show that an increased contrast resolution, higher dynamic range and, consequently, better quality of the obtained images is achieved when using the SMF compared to standard DAS. This technique could be very promising for those applications which suffer from limited image contrast and resolution.

## ACKNOWLEDGMENT

The authors thank Lars N. Moesner, Jan P. Bagge (BK Ultrasound) for producing the interconnect electronics and Christopher Beers (Sound Technology, State College, PA, USA) for designing the array. This work was financially supported

by grant 82-2014-4 from the Danish National Advanced Technology Foundation and from BK Ultrasound ApS, Herlev, Denmark.

## REFERENCES

- [1] O. T. von Ramm, S. W. Smith, and H. G. Pavy, "High speed ultrasound volumetric imaging system – Part II: Parallel processing and image display," *IEEE Trans. Ultrason., Ferroelec., Freq. Contr.*, vol. 38, pp. 109–115, 1991.
- [2] R. E. Davidsen, J. A. Jensen, and S. W. Smith, "Two-dimensional random arrays for real time volumetric imaging," *Ultrasonic Imaging*, vol. 16, no. 3, pp. 143–163, July 1994.
- [3] M. F. Rasmussen and J. A. Jensen, "3-D ultrasound imaging performance of a row-column addressed 2-D array transducer: A measurement study," in *Proc. IEEE Ultrason. Symp.*, July 2013, pp. 1460–1463.
- [4] J. T. Yen, "Beamforming of sound from two-dimensional arrays using spatial matched filters," *J. Acoust. Soc. Am.*, vol. 134, no. 5, pp. 3697–704, 2013.
- [5] A. Sampaleanu, P. Zhang, A. Kshirsagar, W. Moussa, and R. Zemp, "Top-orthogonal-to-bottom-electrode (TOBE) CMUT arrays for 3-D ultrasound imaging," *IEEE Trans. Ultrason., Ferroelec., Freq. Contr.*, vol. 61, no. 2, pp. 266–276, 2014.
- [6] C. E. M. Démoré, A. Joyce, K. Wall, and G. Lockwood, "Real-time volume imaging using a crossed electrode array," *IEEE Trans. Ultrason., Ferroelec., Freq. Contr.*, vol. 56, no. 6, pp. 1252–1261, 2009.
- [7] M. F. Rasmussen, T. L. Christiansen, E. V. Thomsen, and J. A. Jensen, "3-D imaging using row-column-addressed arrays with integrated apodization — Part I: Apodization design and line element beamforming," *IEEE Trans. Ultrason., Ferroelec., Freq. Contr.*, vol. 62, no. 5, pp. 947–958, 2015.
- [8] S. I. Awad and J. T. Yen, "3-D spatial compounding using a row-column array," *Ultrason. Imaging*, vol. 31, no. 2, pp. 120–130, 2009.
- [9] J. A. Jensen and P. Gori, "Spatial filters for focusing ultrasound images," in *Proc. IEEE Ultrason. Symp.*, 2001, pp. 1507–1511.
- [10] J. A. Jensen and N. B. Svendsen, "Calculation of pressure fields from arbitrarily shaped, apodized, and excited ultrasound transducers," *IEEE Trans. Ultrason., Ferroelec., Freq. Contr.*, vol. 39, pp. 262–267, 1992.
- [11] J. A. Jensen, "Field: A program for simulating ultrasound systems," *Med. Biol. Eng. Comp.*, vol. 10th Nordic-Baltic Conference on Biomedical Imaging, Vol. 4, Supplement 1, Part 1, pp. 351–353, 1996.
- [12] T. L. Szabo, *Diagnostic ultrasound imaging: Inside out*, 2nd ed. Elsevier (Oxford, UK), 2014.